



Article scientifique

Article

2019

Accepted version

Open Access

This is an author manuscript post-peer-reviewing (accepted version) of the original publication. The layout of the published version may differ .

Towards early-warning gene signature of *Chlamydomonas reinhardtii* exposed to Hg-containing complex media

Beauvais-Flueck, Rebecca; Slaveykova, Vera; Ulf, Skyllberg; Cosio, Claudia

How to cite

BEAUVAIS-FLUECK, Rebecca et al. Towards early-warning gene signature of *Chlamydomonas reinhardtii* exposed to Hg-containing complex media. In: Aquatic Toxicology, 2019, vol. 214, n° 105259, p. 1–10. doi: 10.1016/j.aquatox.2019.105259

This publication URL: <https://archive-ouverte.unige.ch/unige:122745>

Publication DOI: [10.1016/j.aquatox.2019.105259](https://doi.org/10.1016/j.aquatox.2019.105259)

1
2
3
4 1 **Towards early-warning gene signature of *Chlamydomonas reinhardtii* exposed to Hg-**
5 2 **containing complex media**
6
7 3

8 4 Rébecca Beauvais-Flück¹, Vera I. Slaveykova¹, Skyllberg Ulf², Claudia Cosio^{1*†}
9 5

10 6 ¹Department F.-A. Forel for environmental and aquatic sciences, Earth and Environmental
11 7 Sciences, Faculty of Sciences, University of Geneva, 66, boulevard Carl-Vogt, CH-1211
12 8 Geneva 4, Switzerland.

13 9 ²Department of Forest Ecology and Management, Swedish University of Agricultural
14 10 Sciences, 901 83 Umeå, Sweden

15 11 †present address: Unité Stress Environnementaux et BIOSurveillance des Milieux Aquatiques
16 12 UMR-I 02 (SEBIO), Université de Reims Champagne Ardenne, F-51687 Reims, France.

17 13
18 14 *Corresponding authors: claudia.cosio@unige.ch, claudia.cosio@univ-reims.fr
19 15
20
21
22
23
24
25
26
27
28
29
30
31
32
33
34
35
36
37
38
39
40
41
42
43
44
45
46
47
48
49
50
51
52
53
54
55
56
57
58
59

60
61
62 **16 Abstract**
63

64 17 The potential of using gene expression signature as a biomarker of toxicants exposure was
65 18 explored in the microalga *Chlamydomonas reinhardtii* exposed 2 hours to mercury (Hg) as
66 19 inorganic mercury (IHg) and methyl mercury (MeHg) in presence of copper (Cu) and
67 20 Suwannee River Humic Acid (SRHA). Total cellular Hg (THg = IHg + MeHg) decreased in
68 21 presence of SRHA for 0.7 nM IHg and 0.4 nM MeHg, but increased for 70 nM IHg exposure.
69 22 In mixtures of IHg + MeHg and (IHg or MeHg) + Cu, SRHA decreased THg uptake, except
70 23 for 0.7 nM IHg + 0.4 nM MeHg which was unchanged. In the absence of SRHA, 0.5 μM Cu
71 24 strongly decreased intracellular THg concentration for 70 nM IHg, while it had no effect for
72 25 0.7 nM IHg and 0.4 nM MeHg. The expression of single transcripts was not correlated with
73 26 measured Hg uptake, but a subset of 60 transcripts showed signatures specific to the exposed
74 27 metal(s) and was congruent with exposure concentration. Notably, the range of fold change
75 28 values of this subset correlated with THg bioaccumulation with a two-slope pattern in line
76 29 with $[\text{THg}]_{\text{intra}}/[\text{THg}]_{\text{med}}$ ratios. Gene expression signature seems a promising approach to
77 30 complement chemical analyses to assess bioavailability of toxicants in presence of other
78 31 metals and organic matter.
79
80
81
82
83
84
85
86
87
88

89 32
90 33 Keywords: copper, dissolved organic matter, microalgae, uptake, transcriptomics.
91 34
92
93
94
95
96
97
98
99
100
101
102
103
104
105
106
107
108
109
110
111
112
113
114
115
116
117
118

1. Introduction

For environmental risk assessment, a rapid diagnostic is instrumental to limit pollution impacts. Thus, the development of early warning tools is highly desirable. In this context, managers of ecosystems use ecotoxicology - the study of biota responses to toxicants- to evaluate the level of toxicity of pollution to identify the most efficient actions. Historically ecotoxicology focused on cellular effects, such as growth or photosynthesis efficiency. Recent advances in system biology, notably new genomic sequencing techniques are fundamentally transforming ecotoxicology approach by offering powerful tools to directly detect the earliest stages of the toxicological response including non-models species with unsequenced genomes (Beauvais-Fluck et al., 2016, 2017; Beauvais-Fluck et al., 2018b; Brinke and Buchinger, 2017; Regier et al., 2016). Transcriptomic offers a great potential because it was shown to be efficient for analysis of short-term exposure, more sensitive than classical bioassays (e.g. bioaccumulation or physiological effects) and to correlate with gradients of contaminants in natural waters, as well as to be able to identify toxicant-specific signatures (Dranguet et al., 2017a; Garcia-Reyero et al., 2009; Gomez-Sagasti et al., 2016; Regier et al., 2013a; Yang et al., 2007). Indeed, several toxicological studies were able to differentiate toxicants on the basis of the gene expression profiles in exposed organisms to multiple environmental stressors, offering a more thorough analysis than currently available bioassays (Aardema and MacGregor, 2002; Beauvais-Fluck et al., 2018a; Beauvais-Fluck et al., 2018b; Poynton et al., 2011; Regier et al., 2013a; Waring et al., 2001). Moreover, transcriptomic has the potential of identifying the impact of several stressors in a single analysis and seems hence particularly interesting for *in-situ* analysis characterized by a cocktail of different metals and the presence of organic matter (Almeida et al., 2005; Beauvais-Fluck et al., 2018a; Beauvais-Fluck et al., 2018b; Dondero et al., 2011; Hutchins et al., 2010; Milan et al., 2015; Regier et al., 2016; Villeneuve et al., 2012). However, there is now a need to better evaluate the potential of this tool, in particular its predictive aspects of bioavailability and toxicity to the ecosystem (Fedorenkova et al., 2010). Notably, the connection between gene response and environmental exposure needs to be investigated in more detail.

Mercury (Hg) toxicity and biomagnification in trophic web is a worldwide hazard in aquatic ecosystems (Lavoie et al., 2013). Nonetheless, an efficient early-warning tool to reliably assess Hg bioavailability and its potential impact in natural environments is still missing. Because Hg enters the food web through phytoplankton (Bravo et al., 2014), microalgae are key organisms to assess Hg exposure (Le Faucheur et al., 2014). In the environment, microalgae are exposed to Hg in the presence of other metals and metal binding organic

178
179
180 69 ligands. In aquatic environments Hg occurs as inorganic Hg (IHg) and methyl Hg (MeHg) and
181
182 70 the concentration of total Hg (THg = IHg + MeHg) generally spans between 1 pM to 30 nM,
183
184 71 with MeHg representing 1 to 30% of THg (Bravo et al., 2014; Cossa et al., 2009). Currently,
185
186 72 the European environmental quality standard for freshwater protection is 0.35 nM THg (Crane
187
188 73 and Babut, 2007). What is more, the dissolved organic matter (DOM) present in freshwaters is
189
190 74 considered as an important environmental factor that protects the aquatic primary producers
191
192 75 from metal stress. Indeed DOM functional groups play a key role for the bioavailability of Hg
193
194 76 and MeHg to microalgae by dictating the chemical speciation of Hg (Skyllberg, 2011).
195
196 77 Further, the complex interplay between DOM, Hg and other soft metals, also affects the
197
198 78 impact of Hg on cells by interacting on similar cellular targets and/or indirectly affecting Hg
199
200 79 uptake (Beauvais-Fluck et al., 2018b; Ravichandran, 2004). Because of this complexity, the
201
202 80 impact of DOM is difficult to predict as both increased and decreased Hg uptake in algae have
203
204 81 been reported in the presence of DOM, depending on the algal species, DOM concentration
205
206 82 and composition (Gorski et al., 2008; Le Faucheur et al., 2014; Luengen et al., 2012).
207
208 83 The aim of this study was to investigate the potential of transcriptomic to develop an early-
209
210 84 warning biomarker tool of Hg-exposure in *Chlamydomonas reinhardtii* under
211
212 85 environmentally relevant conditions. Previous analysis revealed that nM concentrations of
213
214 86 IHg and MeHg are sublethal in *C. reinhardtii*, but induced an obvious and efficient defense
215
216 87 response at the gene and cell level (Beauvais-Fluck et al., 2016, 2017). Briefly, both nM IHg
217
218 88 and MeHg increased *chlorophyll a* content and increased photosynthesis efficiency, MeHg
219
220 89 additionally increased intracellular reactive oxygen species (ROS) concentration and
221
222 90 regulated a higher number of genes than IHg (Beauvais-Fluck et al., 2016, 2017). As toxic
223
224 91 metals generally occur in mixtures in the aquatic environment, copper (Cu) was chosen to
225
226 92 study its effect on Hg uptake because of i) its ubiquitous presence in freshwater, ii) its
227
228 93 essentiality (*vs* nonessential Hg) to primary producers and iii) the previous observation of a
229
230 94 competition between Cu and IHg uptake in a cyanobacteria and a macrophyte (Pandey and
231
232 95 Singh, 1993; Regier et al., 2013b). Cu concentrations in aquatic systems have been reported
233
234 96 from 0.4 to 400 μ M, but it's known that its bioavailability and toxicity to organisms are highly
235
236 97 dependent on its chemical speciation (USEPA, 2007; Zhang et al., 2017). We analyzed here
98
99 the regulation of a subset of transcripts and linked transcript expression signatures to Hg
100
101 intracellular concentrations, used as a direct measure of Hg bioavailability, in microalgae
exposed to nM concentrations inorganic Hg (IHg) and/or methyl Hg (MeHg) in complex
media including an essential metal (i.e. Cu) and humic substances (as proxy for the

237
238
239 102 recalcitrant component of DOM). In addition the influence of IHg and MeHg on the gene
240
241 103 expression triggered by Cu exposure was also considered.
242
243 104

244 105 **2. Material and methods**

247 107 *2.1. Experimental design*

248
249 108 Based on the global transcriptional analysis (RNA-Seq) of *Chlamydomonas reinhardtii* to
250
251 109 IHg, MeHg and Cu in single exposure (Beauvais-Fluck et al., 2016, 2017), a subset of
252
253 110 transcripts showing a specific response or a dose-dependent response to IHg, MeHg or Cu
254
255 111 were selected. Suwannee River Humic Acid (SRHA) standard (International Humic
256
257 112 Substances Society, St. Paul, MN, USA) was used as a proxy for the more recalcitrant fraction
258
259 113 of DOM. We tested 0.7 or 70 nM IHg, 0.4 nM MeHg and IHg-MeHg mixtures (ratios
260
261 114 IHg:MeHg of 1.75 or 175), in the presence or absence of 0.5 μM Cu and of SRHA (1 or 10
262
263 115 $\text{mg}\cdot\text{L}^{-1}$) to mimic conditions likely to be found in a Hg-contaminated site.
264

263 117 *2.2. Labware*

265 118 All material was washed in 10% HNO_3 (EMSURE, Merck, Darmstadt, Germany) followed by
266
267 119 two 10% HCl acid baths (EMSURE, Merck, Darmstadt, Germany), thoroughly rinsed with
268
269 120 ultrapure water (MilliQ Direct system, Merck, Darmstadt, Germany) and dried under a
270
271 121 laminar flow hood. Material for culture and experiments, including media, were additionally
272
273 122 autoclaved (1 bar, 121°C , 20 min) to avoid microbial contamination.
274

274 124 *2.3. Exposure of algae*

276 125 *Chlamydomonas reinhardtii* (wild type strain CPCC11, Canadian Phycological Culture
277
278 126 Centre, Department of Biology, University of Waterloo, Waterloo, ON, Canada) were
279
280 127 harvested in their mid-exponential growth phase and exposed in 100 mL of an artificial
281
282 128 medium, containing $8.2\cdot 10^{-4}$ M CaCl_2 , $3.6\cdot 10^{-4}$ M MgSO_4 , $2.8\cdot 10^{-4}$ M NaHCO_3 , $1.0\cdot 10^{-4}$ M
283
284 129 KH_2PO_4 and $5.0\cdot 10^{-6}$ M NH_4NO_3 , pH was 6.9 ± 0.1 . The cell density was $8.1 \pm 1.1\cdot 10^5$
285
286 130 $\text{cell}\cdot\text{mL}^{-1}$. All exposures were conducted using three biological replicates. The exposure
287
288 131 duration of 2 h was chosen based on previous data of Hg toxicokinetics and *in-situ* RNA-Seq
289
290 132 that supported the interest of such length of exposure in the field because it allows targeting
291
292 133 early-response genes that are more specific to the toxicant than latter gene response
293
294 134 (Beauvais-Fluck et al., 2016; Dranguet et al., 2017a).
295

296
297
298 135 For uptake experiments, exposure medium was prepared and enriched (or not) with SRHA 24
299
300 136 h before the exposure experiment, while metals were added 30 min before algae. *C.*
301 137 *reinhardtii* cells were exposed or not (control) 2 h to 0.7 or 70 nM IHg (Hg(NO₃)₂ standard
302
303 138 solution, Sigma-Aldrich, Buchs, Switzerland), 0.4 nM MeHg (MeHgCl standard solution,
304
305 139 Alfa Aesar, Ward Hill, MA, USA) or 0.5 μM Cu (CuSO₄ solution, Sigma-Aldrich, Buchs,
306
307 140 Switzerland) and the following mixtures: 0.7 nM IHg + 0.4 nM MeHg, 70 nM IHg + 0.4 nM
308
309 141 MeHg, 0.7 nM IHg + 0.5 μM Cu, 70 nM IHg + 0.5 μM Cu and 0.4 nM MeHg + 0.5 μM Cu,
310
311 142 (without SRHA), 1 mg·L⁻¹ SRHA or 10 mg·L⁻¹ SRHA.
312
313 143

314 144 2.4. *Metal Uptake*

315 145 After exposure, cells (50 mL) were centrifuged (10 min, 1300g). Pellets of algae exposed to
316 146 IHg or MeHg and Cu were resuspended in 1 mM ethylene-diamine-tetraacetic-acid (EDTA,
317 147 Sigma-Aldrich, Buchs, Switzerland) + 1 mM cysteine (Sigma-Aldrich, Buchs, Switzerland)
318 148 and 1 mM EDTA, respectively and centrifuged (10 min, 1300g). Both washing media were
319 149 prepared with the metal-free exposure medium. This procedure eliminated metals loosely
320 150 bound to cell walls to enable measure of intracellular metal concentration ([metal]_{intra}). Algal
321 151 pellets were immediately freeze-dried (Beta 1-8 K, Christ, Germany).

322 152 Intracellular total Hg (THg = IHg + MeHg) concentration was determined on freeze-dried
323 153 pellets by atomic absorption spectrometry using the Advanced Hg Analyzer AMA 254 (Altec
324 154 s.r.l., Czech Republic). The detection limit (DL) defined as 3× the standard deviation (SD) of
325 155 10 blank measurements was 0.05 ng THg. The accuracy of the measurements was examined
326 156 by certified reference material (CRM) MESS-3, showing 100 ± 0.1 % recovery. To measure
327 157 Cu uptake, dry algal pellets were digested in 1 mL HNO₃ (Suprapur, Merck Darmstadt,
328 158 Germany) at 90 °C for 1 h and Cu concentration was measured by inductively coupled plasma
329 159 mass spectrometry (ICP-MS; 7700x, Agilent Technologies, Morges, Switzerland) which DL
330 160 was 0.18 μg·L⁻¹ Cu.

331 161 Concentrations of THg, MeHg and Cu in media were determined by the MERX Automated
332 162 Total Mercury Analytical System (Brooks Rand Instruments, Seattle, WA, USA), having a
333 163 DL of 0.04 ng·L⁻¹ THg, the MERX Automated Methyl Mercury Analytical System (Brooks
334 164 Rand Instruments, Seattle, WA, USA) having a DL of 0.01 ng·L⁻¹ MeHg and ICP-MS (see
335 165 above), respectively. Effective concentrations in media for single and mixtures metal
336 166 experiments were in average 0.36 ± 0.03 nM MeHg and 0.68 ± 0.02 nM THg for low
337 167 concentration experiments, and 68.0 ± 1.8 nM THg in high concentration experiments. The
338 168 concentration of Cu was in average 0.55 ± 0.004 μM Cu. The chemical speciation of IHg,

355
356
357 169 MeHg, and Cu in media solutions were calculated from finally determined metal
358
359 170 concentrations by an iterative procedure in Excel (Microsoft, Redmond, WA, USA), as
360
361 171 described in (Beauvais-Fluck et al., 2018b).

362 172

363 364 173 *2.5. Transcript response assessment by nCounter*

365 174 The nCounter technology by NanoString Inc. (Seattle, WA, USA) (Geiss et al., 2008), a
366
367 175 medium-throughput quantitative approach to study differential transcript expression, without
368
369 176 the need to perform reverse transcription of mRNA to cDNA and subsequent polymerase
370
371 177 chain reaction (PCR), was chosen to test transcript expression level as biomarker of metal
372
373 178 exposure. A subset of transcripts was selected according to the correlation of their expression
374
375 179 level with intracellular Hg or Cu concentrations in previous RNA-Seq experiment (Table S1)
376
377 180 (Beauvais-Fluck et al., 2017), available in the Gene Expression Omnibus database
378
379 181 (GSE65109). The set included 3 housekeeping transcripts (for input variation), 6 positive (for
380
381 182 lane specific variation) and 8 negative (for background correction) internal controls. Total
382
383 183 RNA was extracted from 50 mL of culture as previously described using TRI Reagent
384
385 184 (Sigma-Aldrich, Buchs, Switzerland) (Beauvais-Fluck et al., 2016, 2017) and 500 ng RNA
386
387 185 were used for nCounter analysis. After background correction and normalization, 5 transcripts
388
389 186 were not further considered because of their too low signal, 192 transcripts passed quality
390
391 187 controls (Table S1), including 122 transcripts not having and 70 transcripts having an
392
393 188 annotation in the MapMan ontology (Thimm et al., 2004). Among the represented metabolic
394
395 189 pathways, 9 transcripts were annotated to the ‘cell’ category (e.g. motility and development),
396
397 190 12 to the ‘transport’ category (including 3 metal transporters, e.g. zinc transport precursor, 1
398
399 191 ammonium and 3 ABC transporters), 7 to the ‘photosynthesis’ category (including 5
400
401 192 transcripts involved in the carbon concentrating mechanism), 7 to the ‘sugar metabolism’
402
403 193 category (glycolysis, TCA, major and minor) and 2 to the ‘tetrapyrrole synthesis’ and to the
404
405 194 ‘oxidation-reduction’ (redox) categories. Other categories (e.g. hormone, secondary
406
407 195 metabolism, lipid, nitrate and biodegradation of xenobiotics) were represented by 1 transcript
408
409 196 each. The category ‘regulation of gene expression’ (i.e. RNA, protein, amino acid, nucleotide,
410
411 197 signaling) included 23 transcripts and 3 transcripts were attributed to the ‘miscellaneous’
412
413 198 category in the codeset (Table S1).

405 199

406 407 200 *2.6. Data analysis*

408 201 Background THg and Cu concentrations in cells measured in the absence of SRHA and in
409
410 202 presence of 1 mg·L⁻¹ SRHA or 10 mg·L⁻¹ SRHA were subtracted from data on metal uptake

203 and t-tests ($\alpha=0.05$) were used to compare metal uptake for each treatment *vs* Control. To
204 compare the different treatments, uptake was normalized by the effective exposure
205 concentration in media at the beginning of treatment ($[\text{metal}]_{\text{intra}}/[\text{metal}]_{\text{med}}$).

206 Fold changes (FC) for the nCounter analysis were calculated in Excel by comparing
207 expression of transcripts in algae exposed to metal(s) (single and mixture), in absence or
208 presence of 1 and 10 mg·L⁻¹ SRHA and for algae exposed to SRHA alone *vs* control (absence
209 of SRHA and absence of Hg, MeHg or Cu). This enabled to analyze both the molecular
210 effects of metal and SRHA, and their interactions. Heatmaps were created in Genesis v1.7.7
211 (Institute for Genomics and Bioinformatics, Graz University of Technology, Graz, Austria)
212 (Sturn et al., 2002).

213 Statistical analyses (t-tests, principal component analysis and histograms) and graphical
214 representations were computed in Sigma Plot (Systat Software, San Jose, CA, USA).

215

216 **3. Results**

217 *3.1. Uptake of IHg and MeHg in mixtures of metals*

218 We assessed the Hg uptake by determining the intracellular metal concentrations and by
219 comparing the ratios of intracellular THg concentrations to IHg and MeHg concentrations in
220 the exposure medium (Figure 1A). While the presence of 0.5 μM Cu had no significant effect
221 on THg uptake in mixtures with 0.7 nM IHg or with 0.4 nM MeHg, the THg uptake decreased
222 five times when the concentration of IHg was increased to 70 nM (Figure 1A, Table S2).
223 Importantly, the uptake of MeHg was much more efficient than uptake of Hg, as revealed by
224 the ratio $[\text{THg}]_{\text{intra}}/[\text{THg}]_{\text{med}}$ being 19 \times higher for 0.4 nM MeHg than that for 0.7 nM IHg
225 solutions.

226 The presence of SRHA had variable effects on THg uptake depending on metal composition
227 (Figure 1B, Table S2). The addition of 1 mg·L⁻¹ SRHA decreased THg uptake (for all
228 exposure conditions except 70 nM IHg) as compared to systems with no humic substances. A
229 similar intracellular concentration of THg was determined at 1 and 10 mg·L⁻¹ SRHA for 0.7
230 nM IHg, 70 nM IHg + 0.4 nM MeHg and 70 nM IHg + 0.5 μM Cu. For 0.7 nM IHg + 0.5 μM
231 Cu a significant decrease in THg uptake was observed when SRHA was increased from 1 to
232 10 mg·L⁻¹ (t-tests, p -values <0.01) (Figure 1B, Table S2). To summarize, THg uptake in IHg
233 treatments is decreased by SRHA in presence of Cu (0.7 and 70 nM IHg) or MeHg (70 nM
234 IHg), while THg uptake is unaffected or even increased by SRHA for IHg treatments in
235 absence of Cu and MeHg. In MeHg treatments THg uptake is generally not affected by Cu,
236 IHg or SRHA. Although some of the results may be explained by uptake being controlled by

237 chemical speciation and metal competition for uptake sites (Table S3), the general picture
238 points at other mechanisms being of major importance for metal uptake in this organism.

239

240 3.2. Transcript signatures of IHg and MeHg alone and with SRHA

241 The expression level of the 192 transcripts strongly changed between the 27 experimental
242 treatments (Table S1). A closer look at the log₂FC values of IHg and MeHg in single
243 exposure, revealed 25 transcripts showing contrasted regulation for 0.7, 70 nM IHg and 0.4
244 nM MeHg (Table 1). Transcript expression was also affected by the presence of SRHA and its
245 concentration. For instance, log₂FC values of the transcript Cre10.g447800, coding for an
246 uncharacterized protein, decreased from 3.5 to 1.9 and 0.5 at 0.7 nM IHg with 0, 1 and 10
247 mg·L⁻¹ SRHA, respectively. A transcript involved in signaling (Cre16.g668850) showed
248 opposite regulation of log₂FC for 0.7 nM (e.g. -4.0 at 0 mg·L⁻¹ SRHA) and 70 nM IHg (e.g.
249 0.6 at 0 mg·L⁻¹ SRHA). In line with the significant decrease in THg uptake for MeHg at 1
250 mg·L⁻¹ SRHA, the expression of g18130 was 1.2× lower at 1 mg·L⁻¹ SRHA. Furthermore, an
251 amino acid transporter (Cre06.g298750) was up-regulated in 0.7 nM and 0.7 nM IHg + 1
252 mg·L⁻¹ SRHA, and down-regulated in the other treatments (Table 1). This transcript could be
253 an interesting candidate biomarker of IHg exposure in the nM range. Two transcripts, g6368
254 showing sequence similarity to the *Arabidopsis thaliana* MLO1 (putatively involved in the
255 modulation of pathogen defense and leaf cell death) and g16833 (involved in post-
256 translational modification), were specifically up-regulated by MeHg, and could thus be
257 interesting candidate biomarkers of MeHg exposure. The expression of the 25 selected
258 transcripts (Table 1) revealed that globally their expression level at 70 nM IHg was closer to
259 0.4 nM MeHg than to 0.7 nM IHg treatment, suggesting that single transcript responses could
260 differentiate IHg exposure at the nM vs the μM range, but not IHg from MeHg in *C.*
261 *reinhardtii*.

262 In the absence of SRHA, the expression of 23 and 15 transcripts (out of 25) was either
263 unchanged or close to the arithmetical mean of their expression in the single IHg and MeHg
264 treatments at 0.7 nM IHg + 0.4 nM MeHg and 70 nM IHg + 0.4 nM MeHg, respectively. At
265 0.7 nM IHg + 0.4 nM MeHg, 2 transcripts showed stronger regulation than at 0.7 nM IHg. At
266 70 nM IHg + 0.4 nM MeHg, the expression of 6 transcripts was stronger than in 70 nM IHg
267 and 4 transcripts had an opposite regulation than in single IHg and MeHg treatments. Data
268 suggested a higher and more specific transcript expression regulation by the interaction of IHg
269 and MeHg when exposed in the 175 IHg:MeHg ratio treatment than in quasi-equimolar
270 treatment.

532
533
534 271 The presence of SRHA had no effect on the transcript expression for 11 and 8 transcripts (4
535 were common) for 0.7 nM IHg + 0.4 nM MeHg and 70 nM IHg + 0.4 nM MeHg,
536 272 respectively. For instance, the expression of Cre02.g109650, coding for a transcript involved
537 273 in the cell motility, was always close to the arithmetical mean of single treatments, at all
538 274 SRHA concentration tested here. On the opposite, the comparison of the expression of 3 and 4
539 275 transcripts to their expressions in single treatments differed in the three SRHA conditions, for
540 276 0.7 nM IHg + 0.4 nM MeHg and 70 nM IHg + 0.4 nM MeHg, respectively. These results
541 277 suggest that SRHA had a significant impact on transcript expression, in single treatments but
542 278 also in IHg-MeHg mixture, supporting that gene expression is a very sensitive variable.
543 279
544 280

550 281 *3.3. Linking single transcript expression level and Hg intracellular concentrations*

551 282 Here we aimed to assess the potential of developing a biomarker of Hg uptake based on
552 283 transcripts' expression level. We thus selected transcripts showing the same \log_2FC signs
553 284 among all IHg and MeHg treatments, resulting in a list of 11 candidate transcripts (Figure 2).
554 285 Both FC and THg uptake were normalized by their values in absence of SRHA to compare all
555 286 treatments, including mixtures with Cu and to account for the effect of SRHA (see above and
556 287 Table S1). Only one transcript, g18130 (kinase) showed a decrease in transcript expression
557 288 level with decreased uptake at 0.7 nM IHg, while the 10 other transcripts resulted in no
558 289 obvious correlation, suggesting that this approach may not be very promising to predict Hg
559 290 uptake in *C. reinhardtii*.
560 291

566 292 *3.4. Linking multiple transcript expression signatures and Hg intracellular* 567 293 *concentrations*

568 294 Here, to assess the potential of transcript expression signature, we selected 60 transcripts for
569 295 further investigation as biomarkers of metal uptake in all experimental treatments. Selection
570 296 of transcripts was made on following criteria: i) transcripts showing a \log_2FC lower than -0.5
571 297 or higher than +0.5 in the '1 mg·L⁻¹ SRHA' and '10 mg·L⁻¹ SRHA' treatments were excluded
572 298 to limit SRHA background signal; ii) the transcripts showing specific expression for 0.7 nM
573 299 IHg, 70 nM IHg and MeHg and different expression level for mixtures with Cu were
574 300 included, iii) transcripts that showed an altered expression with SRHA congruent with
575 301 measured uptake were selected. Principal component analysis (Figure S1) showed that the
576 302 signature of this subset of transcripts efficiently discriminated 0.7 nM IHg (and 0.7 nM + 0.4
577 303 nM MeHg) from 70 nM IHg (and 0.7 nM IHg + 0.4 nM MeHg), and to a lesser extent 0.4 nM
578 304 MeHg from 70 nM IHg. The heatmap built with all the treatments showed similar outcomes
579
580
581
582
583
584
585
586
587
588

591
592
593 305 as the principal component analysis (Figure 3, clusters A and C). Mixtures of IHg with Cu
594 306 (cluster D) were clustered separately from Cu alone (0 and 1 mg·L⁻¹ SRHA, cluster E) and
596 307 IHg alone (clusters A and C).

598 308 The signature of the subset of transcripts also allowed classifying samples according to Hg
599 309 uptake: e.g. 0.7 nM IHg + 10 mg·L⁻¹ SRHA (0.003 ± 0.015 amol_{THg}·cell⁻¹) was closer to the
601 310 signatures of SRHA than to 0.7 nM IHg + 10 mg·L⁻¹ SRHA (0.012 ± 0.015 amol·cell⁻¹). In
602 311 cluster A, the samples classified according to measured [THg]_{intra}, ranging from 17.2 to 9.5
603 312 amol_{THg}·cell⁻¹ from 70 nM IHg + 10 mg·L⁻¹ SRHA to 70 nM + 0.4 nM MeHg + 10 mg·L⁻¹
605 313 SRHA, respectively. We observed the same trend in cluster E, ranging from 2.47 amol_{THg}·cell⁻¹
607 314 to 0 amol_{THg}·cell⁻¹ (i.e. below background THg concentration in 10 mg·L⁻¹ SRHA) from 70
609 315 nM IHg + 0.5 μM to 0.7 nM IHg + 0.5 μM + 10 mg·L⁻¹ SRHA.

611 316 Five transcripts, that showed a strong down-regulation in Cu only treatment, were included in
612 317 the subset of transcripts and successfully discriminated a specific signature for Cu treatments.
613 318 The signature of transcripts exposed to Cu + 10 mg·L⁻¹ SRHA was, however, close to the
615 319 signature of SRHA, in line with the strong effect of SRHA on Cu uptake (see below).

617 320 As mentioned above, among the 192 transcripts studied by nCounter, we could identify few
618 321 transcripts discriminating, 0.7 nM IHg, 70 nM IHg and 0.4 nM MeHg (Table 1), but their FC
619 322 were not congruent with THg uptake (Figure 2). On the other hand, when plotting the
620 323 distribution of log₂FC values for the 60 selected transcripts for all treatments including 1 and
621 324 10 mg·L⁻¹ SRHA (Figures S2), we found the number of transcripts with high FC value to
622 325 increase with increased intracellular concentration. We thus plotted the range of log₂FC
623 326 values (difference between the lowest and the highest log₂FC values) and THg uptake
624 327 normalized by the concentration of exposure ([THg]_{intra}/[THg]_{med} ratio) for the 60 selected
625 328 transcripts (Figure 4). A linear relationship was observed for 0.7 nM IHg and 0.7 nM IHg +
626 329 0.5 μM Cu (lower [THg]_{intra}/[THg]_{med} ratio) (adjusted R² = 0.84) and another linear
627 330 relationship for 70 nM IHg, 70 nM + 0.4 nM MeHg and 0.4 nM MeHg, in line with their
628 331 higher [THg]_{intra}/[THg]_{med} ratios (adjusted R² = 0.92) (Figure 4). Correlations were slightly
629 332 weaker when 0.7 nM IHg + 0.4 nM MeHg or 0.4 nM MeHg + 0.5 μM Cu were included
630 333 respectively with the lower [THg]_{intra}/[THg]_{med} ratio (adjusted R² = 0.58). However, this linear
631 334 correlation between transcript expression and Hg uptake appears to be promising for the
632 335 further development of transcriptomic tools to assess Hg exposure and Hg bioavailability in
633 336 mixtures.

634 337

635 338 3.5. *Copper uptake and transcript expression in response to Cu exposure*

650
651
652 339 For comparative purpose, we assessed the transcript expression and Cu uptake in complex
653
654 340 media containing Cu. In the absence of SRHA, Cu intracellular concentration decreased in
655
656 341 mixture with 70 nM IHg (2×) and 0.4 nM MeHg (1.7×) treatments, while it was unchanged in
657
658 342 mixture with 0.7 nM IHg (Table S2). The presence of SRHA significantly decreased Cu
659
660 343 uptake in all conditions (t-tests, p -values<0.01) (Table S2). More in detail, for the 0.5 μM Cu,
661
662 344 Cu uptake decreased (1.9×) from 0 mg·L⁻¹ SRHA to 1 mg·L⁻¹ SRHA, but was unchanged
663
664 345 from 1 to 10 mg·L⁻¹ SRHA, while Cu intracellular concentration further decreased (2.2×) at
665
666 346 10 mg·L⁻¹ SRHA for 0.7 nM IHg + 0.5 μM Cu. For both 70 nM IHg + 0.5 M Cu and 0.4 nM
667
668 347 MeHg + 0.5 μM Cu treatments, measured intracellular concentrations in the presence of 10
669
670 348 mg·L⁻¹ SRHA were below the background concentration of control cells exposed to 10 mg·L⁻¹
671
672 349 SRHA (Table S2). These results imply that MeHg and SRHA have a strong negative effect on
673
674 350 Cu uptake and that Cu in mixture with high IHg concentration affected both THg and Cu
675
676 351 uptake in *C. reinhardtii*. The decrease of Cu uptake with increasing SRHA concentration was
677
678 352 in fair agreement with a modeled decreased fraction of inorganic Cu, whereas negative
679
680 353 impacts of Hg and MeHg on Cu uptake likely have little to do with competition given the
681
682 354 large differences in concentrations (Tables S2 and S3).

678 355 Exposure to Hg, Cu and SRHA resulted in a wide range of Cu intracellular concentrations.
679
680 356 For comparison, we plotted transcript FC values against Cu intracellular concentrations and
681
682 357 found 7 transcripts showing dose-dependent response with Cu uptake in the studied mixtures
683
684 358 (Figure S3). For instance, log₂FC increased with increased uptake for the antioxidant enzyme
685
686 359 glutathione peroxidase 5 (GPX5, Cre10g.458450), while log₂FC decreased for Cre14.g615350
687
688 360 involved in oxygen transport. The Fe-assimilating protein (Cre12.g456600) showed a bell
689
690 361 shape with increasing uptake of Cu. Data suggest that single transcript expression could
691
692 362 assess more reliably Cu bioavailability than Hg bioavailability. However, both Hg
693
694 363 bioavailability and Cu bioavailability were well correlated with transcript expression
695
696 364 signature (see above).

694 365

695 366 **4. Discussion**

697 367 *4.1. Impact of DOM on Hg and Cu uptake*

698 368 We hypothesized that the presence of SRHA would decrease Hg, MeHg and Cu uptake and
699
700 369 consequently impact the level of transcript regulation. In agreement with the above
701
702 370 hypothesis, addition of SRHA decreased THg intracellular concentration in 0.4 nM MeHg
703
704 371 treatments as well as Cu intracellular concentration in all treatments. The latter observation
705
706 372 was consistent with the decrease of metal uptake in presence of DOM observed for many

709
710
711 373 cations, e.g. Cu^{2+} and Cd^{2+} , and was attributed to the complexation of metals to DOM binding
712 374 sites, such as oxygen-containing, amino and reduced sulfur functional groups, reducing the
713 375 free metal ions concentrations and thus metal bioavailability (Lamelas and Slaveykova, 2007).
714 376 It has been reported that DOC concentrations exceeding 100 μM decreased IHg and MeHg
715 377 uptake in the diatom *Thalassiosira pseudonana* when exposed 1 h to natural waters spiked
716 378 with 2 nM IHg or 0.9 nM MeHg (Zhong and Wang, 2009). Similarly, in the diatom *Cyclotella*
717 379 *meneghiniana*, exposure during 72 h to 0.4-0.8 nM MeHg with increasing DOM
720 380 concentration (0, 1.5, 3, 5, 10 and 20 $\text{mg}\cdot\text{L}^{-1}$ DOM isolated from natural waters) showed a
721 381 decrease of MeHg uptake (Luengen et al., 2012). For the green alga *Selenastrum*
722 382 *capricornutum*, additions of 10-20 $\text{mg}\cdot\text{L}^{-1}$ DOM decreased IHg and MeHg uptake after 24 h
723 383 of exposure to 1 pM IHg and 3 pM MeHg (Gorski et al., 2008). A recent study further
724 384 demonstrated that THg uptake in biofilms correlated with the predicted concentrations of IHg
725 385 chemical species not bound to organic ligands in natural waters (Dranguet et al., 2017b). In
726 386 contrast, THg uptake by *C. reinhardtii* in our study increased after addition of 10 $\text{mg}\cdot\text{L}^{-1}$
727 387 SRHA at 70 nM IHg. A doubling of MeHg uptake was reported in *C. reinhardtii* exposed to
728 388 0.6-0.7 nM MeHg with increased DOC (280 μM DOC vs 177 μM DOC) (Pickhardt and
729 389 Fisher, 2007). Using a bacterial bioreporter it was observed that IHg bioavailability under
730 390 non-equilibrium conditions significantly increased when the DOM concentration was
731 391 increased from 0 to 10 $\text{mg}\cdot\text{L}^{-1}$ DOM, but the bioavailability declined upon further increase in
732 392 DOM to 50 $\text{mg}\cdot\text{L}^{-1}$ (Chiasson-Gould et al., 2014). To summarize, despite many observations
733 393 providing support for binding to DOM and competition with other metals being in control of
734 394 IHg and MeHg uptake by organisms in natural waters, there are also results pointing at more
735 395 complicated explanations. In this study the modeled chemical speciation of IHg, MeHg and
736 396 Cu (dividing each metal into fractions involving organic and inorganic ligands; Table S3) is
737 397 difficult to directly link with their bioavailability (Table S2), suggesting that other
738 398 mechanisms are interfering.

739 399 We recently studied the impact on THg intracellular concentration of SRHA in the aquatic
740 400 macrophyte *Elodea nuttallii* using similar experimental conditions as reported here (Beauvais-
741 401 Fluck et al., 2018b). While addition of 1 $\text{mg}\cdot\text{L}^{-1}$ SRHA had no impact on uptake, an increase
742 402 to 10 $\text{mg}\cdot\text{L}^{-1}$ SRHA significantly decreased THg intracellular concentrations in both IHg and
743 403 MeHg 0.1 nM treatments. An increase of IHg to 10 nM had no further increasing effect on
744 404 THg intracellular concentration. For both IHg + MeHg and IHg + Cu, addition of 10 $\text{mg}\cdot\text{L}^{-1}$
745 405 SRHA significantly reduced THg intracellular concentration (as compared to control and 1
746 406 $\text{mg}\cdot\text{L}^{-1}$), whereas for the MeHg + Cu mixture THg intracellular concentrations increased by

768
769
770 407 1.9× concomitantly with a 1.4× decrease in Cu intracellular concentrations. Based on
771
772 408 speciation modeling, it was suggested that formation of Cu(I) in presence of *E. nuttallii* could
773
774 409 explain these data together with the established difference in binding affinities for IHg and
775
776 410 MeHg to DOM functional groups. These very clear differences in the uptake of IHg, MeHg
777
778 411 and Cu between *E. nuttallii* and *C. reinhardtii* could be attributed to the unicellularity of the
779
780 412 alga vs. the pluricellularity of the macrophyte. Another factor that differed between these two
781
782 413 experiments is the surface-to-volume ratio which is expected to result in higher uptake in
783
784 414 unicellular organisms (Beauvais-Fluck et al., 2018a). However, in contrast to this expectation,
785
786 415 THg intracellular concentrations in *E. nuttallii* appeared to be higher than for *C. reinhardtii*,
787
788 416 in line with field observations showing a high Hg uptake in *E. nuttallii* compared to other
789
790 417 primary producers (Beauvais-Fluck et al., 2018a). Besides, based on transcriptome responses,
791
792 418 the impact of IHg and MeHg uptake appears to be lower for *C. reinhardtii* than for *E. nuttallii*
793
794 419 both in controlled and field experimental conditions (Beauvais-Fluck et al., 2018a; Dranguet
795
796 420 et al., 2017a). Although *C. reinhardtii* harvests light via chloroplasts for energy as plants do,
797
798 421 it also possesses numerous genes derived from the last plant-animal common ancestor that
799
800 422 have been lost in angiosperms, including transporters and the possibility of extensive
801
802 423 metabolic flexibility (Merchant et al., 2007). Taken together, our divergent observations on
803
804 424 how an unicellular and a pluricellular organism take up IHg, MeHg and Cu may imply that
805
806 425 homeostasis networks triggered by IHg, MeHg and Cu exposure are species-specific and
807
808 426 modify the metal uptake by different organisms to an extent that chemical speciation
809
810 427 modeling alone cannot explain.

804 428 805 429 *4.2. Impact of Cu on Hg uptake and impact of Hg on Cu uptake*

807 430 In aquatic ecosystems, toxicants are present in cocktails, thus to improve environmental
808
809 431 realism of the exposures, here we further tested the impact of Cu on Hg uptake. We
810
811 432 hypothesized that chemical mixtures will affect metal bioaccumulation, e.g. by direct
812
813 433 competition for uptake or complexation with humic acid, or through synergistic interactions.
814
815 434 We observed a 4.7× decrease of THg uptake in 70 nM IHg + 0.5 μM Cu, but no impact in 0.7
816
817 435 nM IHg + 0.5 μM Cu treatment. Concomitantly, we observed a 2x decreased Cu uptake in 70
818
819 436 nM IHg + 0.5 μM Cu treatment. In the cyanobacteria *Nostoc calcicola*, mixture exposure of
820
821 437 1.5 μM IHg + 40 μM Cu decreased 2× IHg uptake (Pandey and Singh, 1993). Here Cu
822
823 438 competition is more effective when present in 10-20× excess than in higher excess. This could
824
825 439 be attributed to Cu homeostasis network regulation that triggers different transporters
826
827 440 according to external Cu concentration. This finding is different from previous observations

827
828
829 441 made on the macrophyte *E. nuttallii* which was suggested to take up Hg using high affinity Cu
830
831 442 transporters COPT1 (Regier et al., 2013a). Again, these contrasted results point to species-
832
833 443 specific homeostasis networks triggered by IHg, MeHg and Cu exposure. Obviously, there is
834
835 444 a need to gain fundamental knowledge on how various metals affect the bioavailability of
836
837 445 other metals in different types of organisms.
838

839 447 4.3. Linking transcript expression level and uptake

840 448 A rapid diagnostic of environmental risk is desirable to limit and mitigate pollution impacts.
841
842 449 Transcriptomic was reported to be more sensitive than classical bioassays (e.g. shorter
843
844 450 exposure and low concentrations), and to have the potential of identifying the impact of
845
846 451 several stressors in a single analysis (Dranguet et al., 2017a; Garcia-Reyero et al., 2009;
847
848 452 Gomez-Sagasti et al., 2016; Regier et al., 2013a; Yang et al., 2007). It seems thus a promising
849
850 453 approach in the context of toxicity and risk assessment but requires further testing in more
851
852 454 complex experimental conditions. In this context, we aimed to investigate in detail the
853
854 455 relationship between transcript expression level and exposure in more realistic environmental
855
856 456 scenarios, using Hg uptake as a “proof of concept”. Here, while it was possible to find 4
857
858 457 transcripts among the 192 transcripts discriminating 0.7 nM IHg, 70 nM IHg and 0.4 nM
859
860 458 MeHg (Table 1), only 1 transcript had a regulation pattern significantly correlated in a dose-
861
862 459 dependent manner to THg uptake (Figure 2). In the same line, two recent studies in aquatic
863
864 460 primary producers showed that using single transcript expression is not sufficient as specific
865
866 461 metal biomarker, while the expression signature of a subset of transcripts seems more
867
868 462 promising. Simon *et al.* (2008, 2011) used single transcript expression as biomarker of Cd
869
870 463 exposure in *C. reinhardtii*, first in controlled laboratory conditions and then *in situ* (Simon et
871
872 464 al., 2011; Simon et al., 2008). None of the 9 potential biomarkers of Cd exposure in *C.*
873
874 465 *reinhardtii* tested in binary metal mixtures with Cu or led by quantitative reverse transcription
875
876 466 PCR confirmed their Cd specificity established in single exposure experiments (Hutchins et
877
878 467 al., 2010). On the opposite, in *E. nuttallii* the signature of transcript expression measured by
879
880 468 nCounter analysis after 24 h exposure in IHg + Cd mixture was able to differentiate mixture
881
882 469 of 1 nM IHg + 1 nM Cu from 1 nM IHg + 0.1 nM MeHg and 1 nM IHg alone, confirming the
883
884 470 sensitivity of this approach (Regier et al., 2013a).

877 471 Similarly, here measuring the signature of a subset of transcripts and the number of transcripts
878
879 472 showing high FC values appeared to be a more consistent approach to assess Hg exposure. A
880
881 473 strong correlation was obtained between THg uptake and the range of FC values, including
882
883 474 for treatments resulting in low THg uptake such as in 0.7 nM IHg and complex media
884
885

886
887
888 475 including Cu and SRHA. This is in line with recent transcriptomic studies on *C. reinhardtii*
889
890 476 and *E. nuttallii* exposed 2 h *in situ*, where the number of transcripts with high FC (e.g. >|4|)
891
892 477 was congruent with the gradient of contamination (up to 12 pM THg), although
893
894 478 bioaccumulation of Hg was comparable with the background levels (Dranguet et al., 2017a).
895
896 479 However, here the linear correlation was different for low and high [THg]_{intra}/[THg]_{med} ratios
897
898 480 in our experimental conditions, pointing that transcript expression showed the highest
899
900 481 sensitivity at low Hg concentrations, which are more likely to be found in natural waters and
901
902 482 difficult to assess by classical bioassays.

903
904 483 What is more, we observed here that the transcriptional profiling of the subset of 60 selected
905
906 484 transcripts successfully clustered treatments according to the metal uptake in all experimental
907
908 485 treatments including mixtures. Moreover, it is likely that the specific signatures are linked to
909
910 486 the different mode of action of IHg, MeHg and Cu. The cluster of MeHg, close to 70 nM IHg,
911
912 487 was consistent with a previous study on the whole transcriptome response to IHg and MeHg
913
914 488 in *C. reinhardtii*, showing many common cellular pathways regulated by IHg and MeHg
915
916 489 exposure, suggesting a common mode of action of both Hg forms (Beauvais-Fluck et al.,
917
918 490 2017). Here, our results showed that MeHg and Cu have distinct modes of action as suggested
919
920 491 by the opposite transcript expression signature observed.

921
922 492 For Cu, the intracellular Cu concentration was globally congruent with the modeled free Cu²⁺
923
924 493 concentration in the exposure medium (except in the most complex media; Tables S2 and S3)
925
926 494 and congruent with the expression level of transcripts. On the opposite, data for Hg uptake
927
928 495 were less straightforward than Cu data and confirmed the difficulty to use chemical modeling
929
930 496 to predict Hg bioavailability even in simplified media in the presence of organic matter and
931
932 497 other metals. Our data highlights the need of an accurate measurement of uptake that critically
933
934 498 reflects bioavailability to cells. There is thus a need for novel tools, like transcriptomic,
935
936 499 notably to assess Hg bioavailability for Hg risk assessment. Indeed, transcript expression
937
938 500 signature could be an efficient biomarker of Hg and other contaminants exposure, because the
939
940 501 expression of numerous transcripts depends on the interaction of the toxicant with
941
942 502 intracellular biomolecules. Additionally, using transcript expression signature may be
943
944 503 valuable in the context of risk assessment due to their high sensitivity and mechanistic value
504
505 (Schirmer et al., 2010). In future research, the subset of transcripts needs improvement by
506
507 adding or removing some transcripts as well as testing additional scenarios (e.g. a larger range
508
of IHg, MeHg and DOM concentrations and their binary and ternary mixtures, several time
points) as well as other toxicants and environmental samples. Notably, the effect on the gene
expression level would need to be linked to effects at higher level of biological organization

945
946
947 509 (i.e. individuals, population) to be applicable in risk assessment (Brinke and Buchinger,
948
949 510 2017). However, our data evidenced that using the expression signature of a subset of 60
950
951 511 transcripts was a promising tool to detect exposure to pollutants in *C. reinhardtii*. Notably, the
952
953 512 range of FC values among regulated transcripts might represent a sensitive early-warning
954
955 513 biomarker of exposure at low concentrations.
956
957 514

957 515 **Acknowledgments**

958
959 516 This work was supported by the Swiss National Science Foundation (contracts
960
961 517 205321_138254 and 200020_157173). RBF was supported by the fund Constantin Topali.
962
963 518 The authors thank Drs. Mylène Docquier and Didier Chollet for helping with nCounter
964
965 519 analyses.
966
967 520

966 521 **References**

968 522 Aardema, M.J., MacGregor, J.T., 2002. Toxicology and genetic toxicology in the new era of
969
970 523 "toxicogenomics": impact of "-omics" technologies. Mutation Research-Fundamental and
971
972 524 Molecular Mechanisms of Mutagenesis 499, 13-25. [http://dx.doi.org/10.1016/S0027-](http://dx.doi.org/10.1016/S0027-5107(01)00292-5)
973
974 525 5107(01)00292-5
975
976 526 Almeida, J.S., McKillen, D.J., Chen, Y.A., Gross, P.S., Chapman, R.W., Warr, G., 2005.
977
978 527 Design and calibration of microarrays as universal transcriptomic environmental biosensors.
979
980 528 Comp Funct Genomics 6, 132-137. <http://dx.doi.org/10.1002/cfg.466>
981
982 529 Beauvais-Fluck, R., Slaveykova, V., Cosio, C., 2018a. Molecular effects of inorganic and
983
984 530 methyl mercury in aquatic primary producers: comparing impact to a macrophyte and a green
985
986 531 microalga in controlled conditions. Geosciences 8.
987
988 532 <http://dx.doi.org/10.3390/geosciences8110393>
989
990 533 Beauvais-Fluck, R., Slaveykova, V.I., Cosio, C., 2016. Transcriptomic and physiological
991
992 534 responses of the green microalga *Chlamydomonas reinhardtii* during short-term exposure to
993
994 535 subnanomolar methylmercury concentrations. Environ Sci Technol 50, 7126-7134.
995
996 536 <http://dx.doi.org/10.1021/acs.est.6b00403>
997
998 537 Beauvais-Fluck, R., Slaveykova, V.I., Cosio, C., 2017. Cellular toxicity pathways of
999
1000 538 inorganic and methyl mercury in the green microalga *Chlamydomonas reinhardtii*. Sci Rep 7,
1001
1002 539 8034. <http://dx.doi.org/10.1038/s41598-017-08515-8>
1003
1004 540 Beauvais-Fluck, R., Slaveykova, V.I., Skyllberg, U., Cosio, C., 2018b. Molecular effects,
1005
1006 541 speciation and competition of inorganic and methyl mercury in the aquatic plant *Elodea*
1007
1008 542 *nuttallii*. Env sci technol 52, 8876-8884. <http://dx.doi.org/10.1021/acs.est.8b02124>

- 1004
1005
1006 543 Bravo, A.G., Cosio, C., Amouroux, D., Zopfi, J., Cheualley, P.A., Spangenberg, J.E.,
1007
1008 544 Ungureanu, V.G., Dominik, J., 2014. Extremely elevated methyl mercury levels in water,
1009
1010 545 sediment and organisms in a Romanian reservoir affected by release of mercury from a chlor-
1011
1012 546 alkali plant. *Water Res* 49, 391-405. <http://dx.doi.org/10.1016/j.watres.2013.10.024>
1013
1014 547 Brinke, A., Buchinger, S., 2017. Toxicogenomics in environmental science. *Adv Biochem*
1015
1016 548 *Eng Biotechnol* 157, 159-186. http://dx.doi.org/10.1007/10_2016_15
1017
1018 549 Chiasson-Gould, S.A., Blais, J.M., Poulain, A.J., 2014. Dissolved organic matter kinetically
1019
1020 550 controls mercury bioavailability to bacteria. *Environ Sci Technol* 48, 3153-3161.
1021
1022 551 <http://dx.doi.org/10.1021/es4038484>
1023
1024 552 Cossa, D., Averty, B., Pirrone, N., 2009. The origin of methylmercury in open Mediterranean
1025
1026 553 waters. *Limnol Oceanogr* 54, 837-844. <http://dx.doi.org/10.4319/lo.2009.54.3.0837>
1027
1028 554 Crane, M., Babut, M., 2007. Environmental quality standards for water framework directive
1029
1030 555 priority substances: challenges and opportunities. *Integr Environ Assess Manag* 3, 290-296.
1031
1032 556 https://doi.org/10.1897/IEAM_2006-045.1
1033
1034 557 Dondero, F., Banni, M., Negri, A., Boatti, L., Dagnino, A., Viarengo, A., 2011. Interactions of
1035
1036 558 a pesticide/heavy metal mixture in marine bivalves: a transcriptomic assessment. *BMC*
1037
1038 559 *Genomics* 12, 195. <http://dx.doi.org/10.1186/1471-2164-12-195>
1039
1040 560 Dranguet, P., Cosio, C., Le Faucheur, S., Beauvais-Fluck, R., Freiburghaus, A., Worms,
1041
1042 561 I.A.M., Petit, B., Civic, N., Docquier, M., Slaveykova, V.I., 2017a. Transcriptomic approach
1043
1044 562 for assessment of the impact on microalga and macrophyte of in-situ exposure in river sites
1045
1046 563 contaminated by chlor-alkali plant effluents. *Water Res* 121, 86-94.
1047
1048 564 <http://dx.doi.org/10.1016/j.watres.2017.05.020>
1049
1050 565 Dranguet, P., Le Faucheur, S., Cosio, C., Slaveykova, V.I., 2017b. Influence of chemical
1051
1052 566 speciation and biofilm composition on mercury accumulation by freshwater biofilms. *Environ*
1053
1054 567 *sci. Proc impacts* 19, 38-49. <http://dx.doi.org/10.1039/c6em00493h>
1055
1056 568 Fedorenkova, A., Vonk, J.A., Lenders, H.J.R., Ouborg, N.J., Breure, A.M., Hendriks, A.J.,
1057
1058 569 2010. Ecotoxicogenomics: Bridging the gap between genes and populations. *Environ Sci*
1059
1060 570 *Technol* 44, 4328-4333. <http://dx.doi.org/10.1021/es9037287>
1061
1062 571 Garcia-Reyero, N., Poynton, H.C., Kennedy, A.J., Guan, X., Escalon, B.L., Chang, B.,
572 Varshavsky, J., Loguinov, A.V., Vulpe, C.D., Perkins, E.J., 2009. Biomarker discovery and
573 transcriptomic responses in *Daphnia magna* exposed to munitions constituents. *Environ Sci*
574 *Technol* 43, 4188-4193. <http://dx.doi.org/10.1021/es803702a>
575 Geiss, G.K., Bumgarner, R.E., Birditt, B., Dahl, T., Dowidar, N., Dunaway, D.L., Fell, H.P.,
576 Ferree, S., George, R.D., Grogan, T., James, J.J., Maysuria, M., Mitton, J.D., Oliveri, P.,

1063
1064
1065
1066
1067
1068
1069
1070
1071
1072
1073
1074
1075
1076
1077
1078
1079
1080
1081
1082
1083
1084
1085
1086
1087
1088
1089
1090
1091
1092
1093
1094
1095
1096
1097
1098
1099
1100
1101
1102
1103
1104
1105
1106
1107
1108
1109
1110
1111
1112
1113
1114
1115
1116
1117
1118
1119
1120
1121

577 Osborn, J.L., Peng, T., Ratcliffe, A.L., Webster, P.J., Davidson, E.H., Hood, L., 2008. Direct
578 multiplexed measurement of gene expression with color-coded probe pairs. *Nature Biotechnol*
579 26, 317-325. <http://dx.doi.org/10.1038/nbt1385>

580 Gomez-Sagasti, M.T., Barrutia, O., Ribas, G., Garbisu, C., Becerril, J.M., 2016. Early
581 transcriptomic response of *Arabidopsis thaliana* to polymetallic contamination: implications
582 for the identification of potential biomarkers of metal exposure. *Metallomics* 8, 518-531.
583 <http://dx.doi.org/10.1039/c6mt00014b>

584 Gorski, P.R., Armstrong, D.E., Hurley, J.P., Krabbenhoft, D.P., 2008. Influence of natural
585 dissolved organic carbon on the bioavailability of mercury to a freshwater alga. *Environ*
586 *Pollut* 154, 116-123. <http://dx.doi.org/10.1016/j.envpol.2007.12.004>

587 Hutchins, C.M., Simon, D.F., Zerges, W., Wilkinson, K.J., 2010. Transcriptomic signatures in
588 *Chlamydomonas reinhardtii* as Cd biomarkers in metal mixtures. *Aquat Toxicol* 100, 120-
589 127. <http://dx.doi.org/10.1016/j.aquatox.2010.07.017>

590 Lamelas, C., Slaveykova, V.I., 2007. Comparison of Cd(II), Cu(II), and Pb(II) biouptake by
591 green algae in the presence of humic acid. *Environ Sci Technol* 41, 4172-4178.
592 <http://dx.doi.org/10.1021/es063102j>

593 Lavoie, R.A., Jardine, T.D., Chumchal, M.M., Kidd, K.A., Campbell, L.M., 2013.
594 Biomagnification of mercury in aquatic food webs: a worldwide meta-analysis. *Environ Sci*
595 *Technol* 47, 13385-13394. <http://dx.doi.org/10.1021/es403103t>

596 Le Faucheur, S., Campbell, P.G.C., Fortin, C., Slaveykova, V.I., 2014. Interactions between
597 mercury and phytoplankton: speciation, bioavailability, and internal handling. *Environ Toxicol*
598 *Chem* 33, 1211-1224. <http://dx.doi.org/10.1002/etc.2424>

599 Luengen, A.C., Fisher, N.S., Bergamaschi, B.A., 2012. Dissolved organic matter reduces
600 algal accumulation of methylmercury. *Environ Toxicol Chem* 31, 1712-1719.
601 <http://dx.doi.org/10.1002/etc.1885>

602 Merchant, S.S., Prochnik, S.E., Vallon, O., Harris, E.H., Karpowicz, S.J., Witman, G.B.,
603 Terry, A., Salamov, A., Fritz-Laylin, L.K., Marechal-Drouard, L., Marshall, W.F., Qu, L.-H.,
604 Nelson, D.R., Sanderfoot, A.A., Spalding, M.H., Kapitonov, V.V., Ren, Q., Ferris, P.,
605 Lindquist, E., Shapiro, H., Lucas, S.M., Grimwood, J., Schmutz, J., Cardol, P., Cerutti, H.,
606 Chanfreau, G., Chen, C.-L., Cognat, V., Croft, M.T., Dent, R., Dutcher, S., Fernandez, E.,
607 Fukuzawa, H., Gonzalez-Ballester, D., Gonzalez-Halphen, D., Hallmann, A., Hanikenne, M.,
608 Hippler, M., Inwood, W., Jabbari, K., Kalanon, M., Kuras, R., Lefebvre, P.A., Lemaire, S.D.,
609 Lobanov, A.V., Lohr, M., Manuell, A., Meier, I., Mets, L., Mittag, M., Mittelmeier, T.,
610 Moroney, J.V., Moseley, J., Napoli, C., Nedelcu, A.M., Niyogi, K., Novoselov, S.V., Paulsen,

1122
1123
1124 611 I.T., Pazour, G., Purton, S., Ral, J.-P., Riano-Pachon, D.M., Riekhof, W., Rymarquis, L.,
1125
1126 612 Schroda, M., Stern, D., Umen, J., Willows, R., Wilson, N., Zimmer, S.L., Allmer, J., Balk, J.,
1127
1128 613 Bisova, K., Chen, C.-J., Elias, M., Gendler, K., Hauser, C., Lamb, M.R., Ledford, H., Long,
1129
1130 614 J.C., Minagawa, J., Page, M.D., Pan, J., Pootakham, W., Roje, S., Rose, A., Stahlberg, E.,
1131
1132 615 Terauchi, A.M., Yang, P., Ball, S., Bowler, C., Dieckmann, C.L., Gladyshev, V.N., Green, P.,
1133
1134 616 Jorgensen, R., Mayfield, S., Mueller-Roeber, B., Rajamani, S., Sayre, R.T., Brokstein, P.,
1135
1136 617 Dubchak, I., Goodstein, D., Hornick, L., Huang, Y.W., Jhaveri, J., Luo, Y., Martinez, D.,
1137
1138 618 Ngau, W.C.A., Otilar, B., Poliakov, A., Porter, A., Szajkowski, L., Werner, G., Zhou, K.,
1139
1140 619 Grigoriev, I.V., Rokhsar, D.S., Grossman, A.R., 2007. The *Chlamydomonas* genome reveals
1141
1142 620 the evolution of key animal and plant functions. *Science* 318, 245-250.
1143
1144 621 <http://dx.doi.org/10.1126/science.1143609>
1145
1146 622 Milan, M., Pauletto, M., Boffo, L., Carrer, C., Sorrentino, F., Ferrari, G., Pavan, L.,
1147
1148 623 Patarnello, T., Bargelloni, L., 2015. Transcriptomic resources for environmental risk
1149
1150 624 assessment: a case study in the Venice lagoon. *Environ Pollut* 197, 90-98.
1151
1152 625 <http://dx.doi.org/10.1016/j.envpol.2014.12.005>
1153
1154 626 Pandey, P.K., Singh, S.P., 1993. Hg²⁺ Uptake in a *Cyanobacterium*. *Curr Microbiol* 26, 155-
1155
1156 627 159. <http://dx.doi.org/10.1007/bf01577371>
1157
1158 628 Pickhardt, P.C., Fisher, N.S., 2007. Accumulation of inorganic and methylmercury by
1159
1160 629 freshwater phytoplankton in two contrasting water bodies. *Environ Sci Technol* 41, 125-131.
1161
1162 630 <http://dx.doi.org/10.1021/Es060966w>
1163
1164 631 Poynton, H.C., Lazorchak, J.M., Impellitteri, C.A., Smith, M.E., Rogers, K., Patra, M.,
1165
1166 632 Hammer, K.A., Allen, H.J., Vulpe, C.D., 2011. Differential gene expression in *Daphnia*
1167
1168 633 *magna* suggests distinct modes of action and bioavailability for ZnO nanoparticles and Zn
1169
1170 634 ions. *Environ sci technol* 45, 762-768. <http://dx.doi.org/10.1021/es102501z>
1171
1172 635 Ravichandran, M., 2004. Interactions between mercury and dissolved organic matter--a
1173
1174 636 review. *Chemosphere* 55, 319-331. <http://dx.doi.org/10.1016/j.chemosphere.2003.11.011>
1175
1176 637 Regier, N., Baerlocher, L., Munsterkötter, M., Farinelli, L., Cosio, C., 2013a. Analysis of the
1177
1178 638 *Elodea nuttallii* transcriptome in response to mercury and cadmium pollution: development of
1179
1180 639 sensitive tools for rapid ecotoxicological testing. *Environ Sci Technol* 47, 8825-8834.
640
<http://dx.doi.org/10.1021/es401082h>
641
642 Regier, N., Beauvais-Flück, R., Slaveykova, V.I., Cosio, C., 2016. *Elodea nuttallii* exposure
643
644 to mercury exposure under enhanced ultraviolet radiation: Effects on bioaccumulation,
transcriptome, pigment content and oxidative stress. *Aquat Toxicol* 180, 218-226.
<http://dx.doi.org/10.1016/j.aquatox.2016.10.001>

1181
1182
1183
1184
1185
1186
1187
1188
1189
1190
1191
1192
1193
1194
1195
1196
1197
1198
1199
1200
1201
1202
1203
1204
1205
1206
1207
1208
1209
1210
1211
1212
1213
1214
1215
1216
1217
1218
1219
1220
1221
1222
1223
1224
1225
1226
1227
1228
1229
1230
1231
1232
1233
1234
1235
1236
1237
1238
1239

645 Regier, N., Larras, F., Bravo, A.G., Ungureanu, V.-G., Amouroux, D., Cosio, C., 2013b.
646 Mercury bioaccumulation in the aquatic plant *Elodea nuttallii* in the field and in microcosm:
647 Accumulation in shoots from the water might involve copper transporters. *Chemosphere* 90,
648 595-602. <http://dx.doi.org/10.1016/j.chemosphere.2012.08.043>
649 Schirmer, K., Fischer, B.B., Madureira, D.J., Pillai, S., 2010. Transcriptomics in
650 ecotoxicology. *Anal Bioanal Chem* 397, 917-923. 10.1007/s00216-010-3662-3
651 Simon, D.F., Davis, T.A., Tercier-Waeber, M.L., England, R., Wilkinson, K.J., 2011. *In situ*
652 evaluation of cadmium biomarkers in green algae. *Environ Pollut* 159, 2630-2636. DOI
653 10.1016/j.envpol.2011.05.028
654 Simon, D.F., Descombes, P., Zerges, W., Wilkinson, K.J., 2008. Global expression profiling
655 of *Chlamydomonas reinhardtii* exposed to trace levels of free cadmium. *Environ Toxicol*
656 *Chem* 27, 1668-1675. <http://dx.doi.org/10.1897/07-649.1>
657 Skyllberg, U., 2011. Chemical speciation of mercury in soil and sediment, in: Liu, G., Cai, Y.,
658 O'Driscoll, N. (Eds.), *Environmental Chemistry and Toxicology of Mercury*.
659 <http://dx.doi.org/10.1002/9781118146644.ch7>
660 Sturn, A., Quackenbush, J., Trajanoski, Z., 2002. Genesis: cluster analysis of microarray data.
661 *Bioinformatics* 18, 207-208. <http://dx.doi.org/10.1093/bioinformatics/18.1.207>
662 Thimm, O., Blasing, O., Gibon, Y., Nagel, A., Meyer, S., Kruger, P., Selbig, J., Muller, L.A.,
663 Rhee, S.Y., Stitt, M., 2004. MAPMAN: a user-driven tool to display genomics data sets onto
664 diagrams of metabolic pathways and other biological processes. *Plant J* 37, 914-939.
665 <http://dx.doi.org/10.1111/j.1365-313X.2004.02016.x>
666 USEPA, 2007. Aquatic life ambient freshwater quality criteria- copper. US Environmental
667 Protection Agency, Office of Water, Washington, DC. [https://www.epa.gov/wqc/aquatic-life-](https://www.epa.gov/wqc/aquatic-life-criteria-copper)
668 [criteria-copper](https://www.epa.gov/wqc/aquatic-life-criteria-copper)
669 Villeneuve, D.L., Garcia-Reyero, N., Escalon, B.L., Jensen, K.M., Cavallin, J.E., Makynen,
670 E.A., Durhan, E.J., Kahl, M.D., Thomas, L.M., Perkins, E.J., Ankley, G.T., 2012.
671 Ecotoxicogenomics to support ecological risk assessment: a case study with bisphenol A in
672 fish. *Environ Sci Technol* 46, 51-59. <http://dx.doi.org/10.1021/es201150a>
673 Waring, J.F., Jolly, R.A., Ciurlionis, R., Lum, P.Y., Praestgaard, J.T., Morfitt, D.C., Buratto,
674 B., Roberts, C., Schadt, E., Ulrich, R.G., 2001. Clustering of hepatotoxins based on
675 mechanism of toxicity using gene expression profiles. *Toxicol. Appl. Pharmacol.* 175, 28-42.
676 <http://dx.doi.org/10.1006/taap.2001.9243>
677 Yang, L., Kemadjou, J.R., Zinsmeister, C., Bauer, M., Legradi, J., Muller, F., Pankratz, M.,
678 Jakel, J., Strahle, U., 2007. Transcriptional profiling reveals barcode-like toxicogenomic

1240
1241
1242
1243
1244
1245
1246
1247
1248
1249
1250
1251
1252
1253
1254
1255
1256
1257
1258
1259
1260
1261
1262
1263
1264
1265
1266
1267
1268
1269
1270
1271
1272
1273
1274
1275
1276
1277
1278
1279
1280
1281
1282
1283
1284
1285
1286
1287
1288
1289
1290
1291
1292
1293
1294
1295
1296
1297
1298

679 responses in the zebrafish embryo. *Genome Biol* 8, R227. [http://dx.doi.org/10.1186/gb-2007-](http://dx.doi.org/10.1186/gb-2007-8-10-r227)
680 8-10-r227
681 Zhang, Y., Zang, W., Qin, L., Zheng, L., Cao, Y., Yan, Z., Yi, X., Zeng, H., Liu, Z., 2017.
682 Water quality criteria for copper based on the BLM approach in the freshwater in China.
683 *PLOS ONE* 12, e0170105. <http://dx.doi.org/10.1371/journal.pone.0170105>
684 Zhong, H., Wang, W.X., 2009. Controls of dissolved organic matter and chloride on mercury
685 uptake by a marine diatom. *Environ Sci Technol* 43, 8998-9003.
686 <http://dx.doi.org/10.1021/es901646k>

687
688

689 **Table 1:** Fold changes (log₂FC) of 25 selected transcripts showing differential expression for IHg and MeHg (--N.A.--, not assigned).

Transcript	MapMan category	0.7 nM IHg			70 nM IHg			0.4 nM MeHg					
		SRHA (mg·L ⁻¹)			SRHA (mg·L ⁻¹)			SRHA (mg·L ⁻¹)					
		0	1	10	0	1	10	0	1	10			
Cre10.g447800	--N.A.--		3.48	1.95	0.54	-0.04		0.00	0.20		0.43	0.45	0.34
Cre06.g298750	transport-AA		2.92	1.39	-0.60	-0.37		-0.37	-0.68		-0.49	-0.73	-0.69
Cre02.g074800	--N.A.--		1.01	0.89	0.49		2.48	2.24	1.91		3.08	2.88	2.53
Cre02.g093500	--N.A.--	-0.14		0.03	-0.30		1.54	1.28	1.29		2.95	3.08	3.12
Cre12.g492650	--N.A.--		0.34	-0.34	-0.26		0.87	0.46	0.77		3.04	3.17	3.05
Cre06.g260550	nucleotide		0.92	0.47	-0.07		1.43	1.33	0.90		2.00	1.94	1.74
Cre16.g657200	xenobiotics	-0.10		0.37	0.68		0.78	0.41	0.91		1.22	1.18	1.53
g9144	cell motility	-2.39	-2.51	-2.19	-0.90		-1.21	-1.24			1.69	1.61	1.84
Cre16.g668850	signalling	-4.05	-3.26	-2.01		0.63	0.66	0.22	-0.11		0.11	-0.27	
Cre17.g714300	--N.A.--	-3.26	-2.27	-1.69		0.24	0.13	-0.42	-0.09		0.04	-0.21	
Cre14.g616050	--N.A.--	-2.39	-2.17	-1.44		0.58	0.40	0.05	0.20		0.35		0.07
Cre06.g249500	RNA	-2.19	-1.84	-1.38		0.69	0.41	-0.03		0.29	0.28	-0.06	
Cre10.g442800	transport-misc	-0.69	-0.47	-0.33	-0.47		0.04	0.10	-0.16		-0.06	-0.11	
Cre12.g529450	cell division	-1.03	-0.92	-0.79	-0.44		-0.49	-0.61		0.07	0.01	-0.03	
Cre03.g152750	apoptosis	-0.72	-0.84	-0.86		0.16	-0.45	-0.25		0.23	0.50		0.57
g11558	--N.A.--	-0.80	-0.63	-0.93		0.84	0.36	0.20		0.63	0.49	0.20	
Cre02.g109650	cell motility	-1.52	-1.00	-0.65		1.13	0.73	0.29		0.94	0.96	0.51	
Cre06.g249350	RNA	-1.78	-1.23	-0.87		0.92	0.69	0.24		0.95	0.95	0.60	
Cre10.g441250	--N.A.--	-0.67	-0.71	-0.36	-0.10		0.15	0.15		0.83	0.68	0.63	
g6368	transport-misc		0.03	-0.16	-0.39		0.01	-0.09	-0.21		0.85	0.60	0.45
g16833	proteins		0.05	0.04	0.06	-0.08		-0.20	-0.20		0.46	0.40	0.54
Cre06.g263550	redox	-0.05	-0.24	-0.44		0.27	0.26	0.35		0.86	1.02	0.92	
g18130	proteins	-0.14	-0.09	-0.13		0.46	0.46	0.40		1.09	0.94	0.99	
Cre10.g458450	redox	-0.18	-0.21	-0.16		0.70	0.67	0.63		0.96	1.09	0.84	
g6373	proteins	-0.21	-0.40	-0.55		0.68	0.74	0.58		1.12	0.77	0.86	

690

691

692

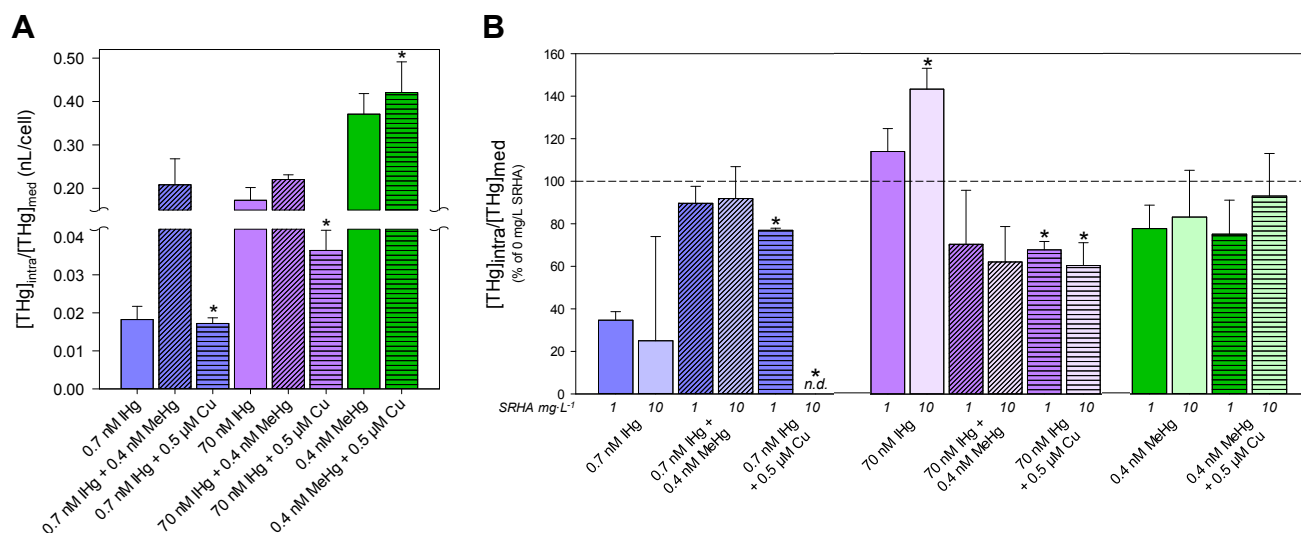


Figure 1: (A) Effect of MeHg on IHg uptake and effect of Cu on IHg and MeHg uptake in absence of SRHA. Asterisks indicate a significant difference with the respective treatment without Cu (t-test, p -value < 0.05). (B) Effect of SRHA on THg uptake for all treatments compared to the respective treatment without SRHA normalized by 100% (dashed line). Asterisks indicate a significant difference with the respective treatment without SRHA (ANOVA post-hoc Holm-Sidak, p -value < 0.05). Uptake was measured as THg (= IHg + MeHg) concentration in algal cells ($[THg]_{intra}$) and divided by concentration in the medium ($[THg]_{med}$) (mean \pm SD, $n = 3$). Numbers 1 and 10 indicate concentration of SRHA ($mg \cdot L^{-1}$).

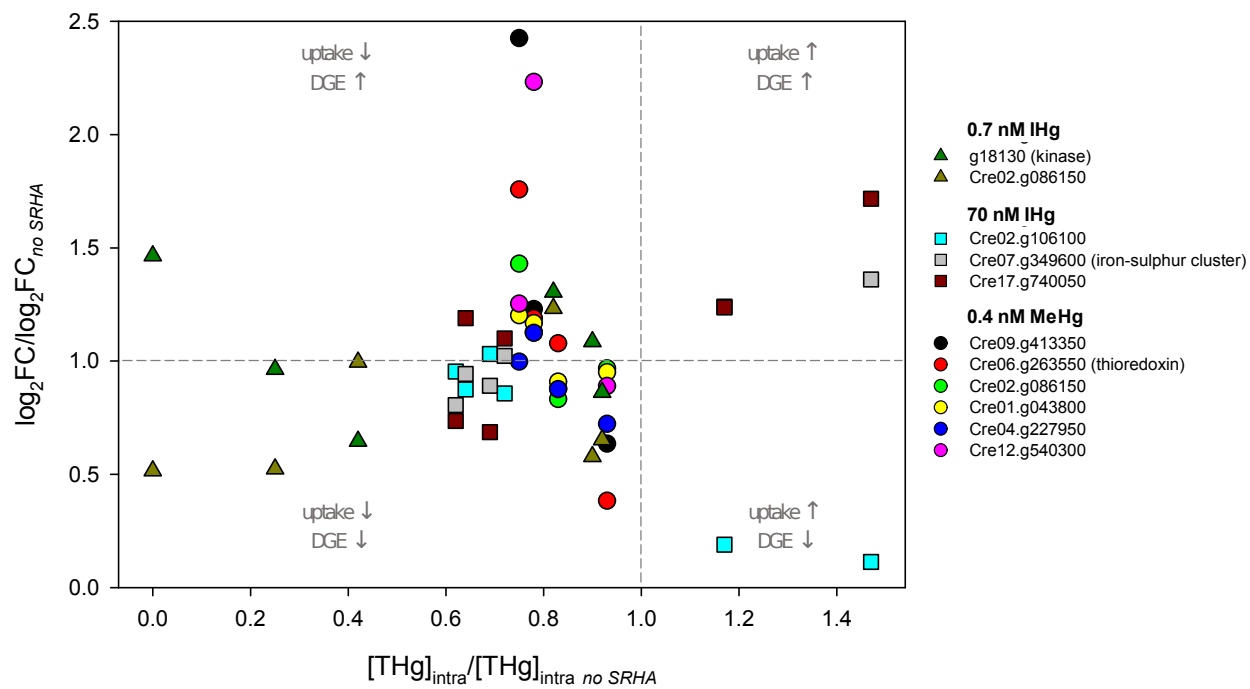


Figure 2: Gene fold changes for 11 selected genes according to THg uptake, both normalized by their value in absence of SRHA.

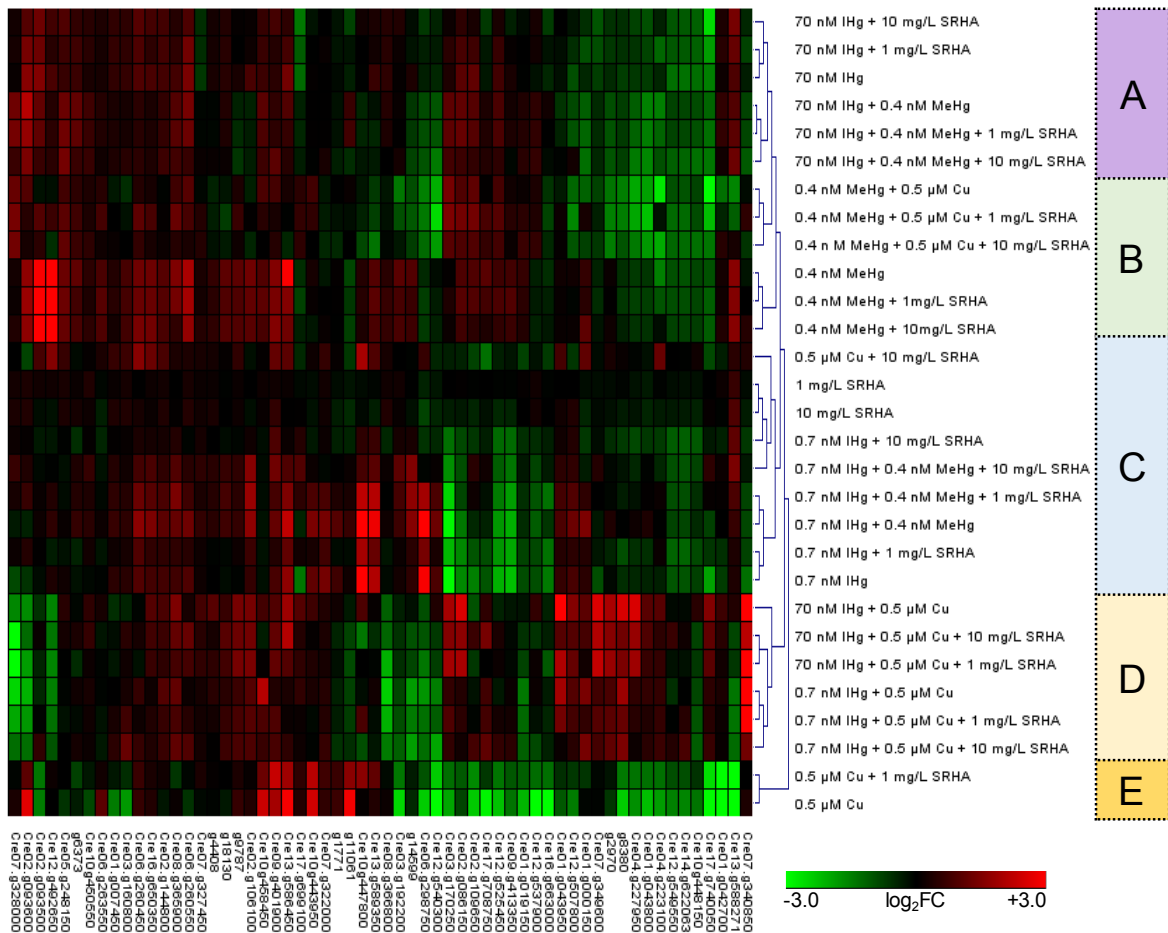


Figure 3: Hierarchical clustering of treatments according to the expression level of 60 selected genes (average linkage, Euclidean distance). Fold changes were calculated by dividing the expression level in the treatment by the expression level in the control (no metal, no SRHA). Letters show second level clusters.

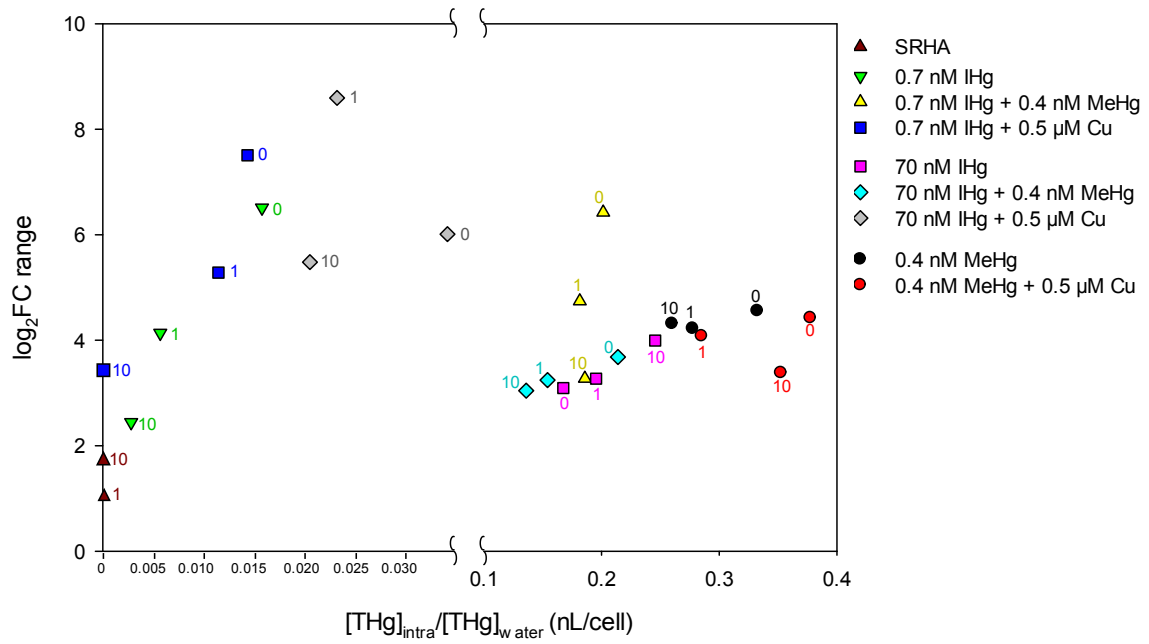


Figure 4: Relationship between the range of \log_2FC values for 60 selected genes (difference between the lowest and the highest \log_2FC values) and THg uptake normalized by medium concentration. Numbers 0, 1 and 10 indicate concentration of SRHA ($\text{mg}\cdot\text{L}^{-1}$).